Clinical and Epidemiologic Research

Downregulation of MST4 Underlies a Novel Inhibitory Role of MicroRNA Let-7a in the Progression of Retinoblastoma

Xinli Zhang, Lili Song, Yanxia Huang, Shaoping Han, Min Hou, and Hongxia Li

Department of Ophthalmology, Luoyang Central Hospital, Luoyang, People's Republic of China

PURPOSE. Retinoblastoma (RB) is the most common intraocular malignancy in children. Deregulation of several microRNAs (miRNAs) has been identified in RB. However, the specific effect of let-7a on RB remains unclear. The present study aims to explore the effect of let-7a on malignant biological behaviors of RB cells and angiogenesis in RB.

METHODS. The expressions of let-7a and mammalian sterile-20 like kinase 4 (MST4) in RB were determined with the use of real-time quantitative polymerase chain reaction (RT-qPCR) and Western blot analysis. Next, in order to explore effects of let-7a and MST4 on RB cellular functions, RB cells were transfected with let-7a-mimic, let-7a inhibitor, si-MST4, or co-transfected with let-7a-mimic and oe-MST4 plasmids. Subsequently, the interaction among let-7a, MST4, and the MAPK signaling pathway was evaluated by RT-qPCR, dual-luciferase reporter gene assay, and Western blot analysis. Finally, the effects of let-7a and MST4 were further confirmed in vivo by injecting nude mice with RB cells stably expressing let-7a agomir or sh-MST4.

RESULTS. Rb tissues and cells presented with downregulated Let-7a and upregulated MST4. Let-7a negatively targeted MST4 to block the activation of the MAPK signaling pathway. Upregulation of let-7a promoted apoptosis, and facilitated proliferation, angiogenesis, migration, and invasion of RB cells by decreasing MST4. Elevation of let-7a or silencing MST4 restricted angiogenesis and tumorigenesis in RB mice.

CONCLUSIONS. Taken together, let-7a inhibits angiogenesis in RB by silencing MST4 and inhibiting the MAPK signaling pathway.

Keywords: microRNA let-7a, MST4, retinoblastoma, angiogenesis, malignant biological behavior, MAPK signaling pathway

Retinoblastoma (RB) is a prototypic genetic cancer that often occurs in children, with about two-thirds of patients diagnosed before 2 years of age and >90% before 5 years old.[1] The initial change that is frequently observed in the tumorigenesis of RB is the suppression of both copies of the RB1 gene and this process holds a great importance in the pathogenesis of RB.[2] Pre-existing profiles on tumor-specific microRNA (miRNA) expression have shown that miRNAs are often aberrantly expressed in various cancers, which could result in cellular transformation and tumorigenesis.[3] Specifically, various cellular damages and pathogenesis signals in multiple types of cells have been found to alter the expression of multiple miRNAs, which often can play important roles in initiation and progression of various cancers.[4]

Mammalian sterile-20 like kinase 4 (MST4) belongs to the sterile 20 serine/threonine kinase family, and changes in its expression level have been reported to be involved in tumorigenicity and androgen receptor status of the cells.[5] A former study found overexpressed MST4 in all pituitary tumor cell types, and silencing MST4 can result in the inhibition of colony formation and proliferation abilities of gonadotrope pituitary tumor cells.[6] According to the Jefferson database (https://cm.jefferson.edu/rna22/Precomputed/?tdsourcetag=s_pctim_aiomsg), MST4 was predicted to be a target gene of let-7a, which has been found as a dysregulated miRNA in RB.[7] In a recent study, it has been reported that let-7a is downregulated in gastric cancer tissues and cell lines.[8] A previous study showed that let-7a was downregulated in nasopharyngeal carcinoma and overexpression of synthetic let-7a leads to inhibited levels of nasopharyngeal carcinoma cell migration and invasion.[9] Sterile 20 kinases are in the upstream in the mitogen-activated protein kinase (MAPK) signaling pathway, which subsequently invokes the MAPKs to activate the MAPKs.[10] Activation of the MAPK/extracellular signal-regulated kinase (ERK) signaling pathway is highlighted as a hallmark of RB.[11] MST4, which is an ERK upstream kinase can activate the oncogenic MAPK signaling pathway.[12] Therefore, on the basis of the above findings, we conducted this study to investigate whether let-7a regulates malignant biological processes of RB cells, such as viability, apoptosis, angiogenesis, migration, and invasion, via MST4-mediated MAPK signaling pathway.

Investigative Ophthalmology & Visual Science

TABLE. Primer Sequences for RT-qPCR

Primer sequence	Forward (5′-3′)	Reverse (5′-3′)
let-7a	CACCCACCACTGGGAGATAAC	TATGGTTGTTCACGACTCCTTCAC
MST4	TTCGAGCTGGTCCATTTGATG	TGAATGCAGATAGTCCAGACCT
U6	CGCAAGGATGACACGCAAAT	TATGGTTGTTCACGACTCCTTCAC
GAPDH	CAGGGCTGCTTTTAACTCTGGT	GATTTTGGAGGGATCTCGCT

GAPDH, glyceraldehyde-3-phosphate dehydrogenase; MST4, Mammalian sterile-20 like kinase 4; RT-qPCR, reverse transcription quantitative polymerase chain reaction.

METHODS

Ethnic Statements

All the guardians of patients and volunteers have signed the informed consent, and this study was carried out in line with the recommendations in the Guide for the Care and Use of Laboratory Animals of the National Institutes of Health. The protocol was approved by the Institutional Animal Care and Use Committee of Luoyang Central Hospital. The animal experiments were conducted with maximum efforts made to minimize pain and number of animals.

Microarray-Based Gene Expression Analysis

RB-related microarray data GSE5222 was obtained from Gene Expression Omnibus (GEO) database (https://www.ncbi.nlm.nih.gov/geo/). The differential expression of genes in GSE5222 was analyzed using the "limma" package with P value < 0.05 and |logFoldChange| > 2 set as the criteria. The upstream miRNA of MST4 and the binding sites of let-7a on MST4 were predicted based on the Jefferson database (https://cm.jefferson.edu/rna22/Precomputed/?tdsourcetag=s_pctim_aiomsg) and the microRNA.org database (http://www.microrna.org/microrna/getMrna.do?gene=51765&utr=2323&organism=9606#hd).

Study Subjects

RB tissues were obtained from 28 patients who had undergone enucleation in Luoyang Central Hospital from February, 2014, to November, 2018. In addition, normal retinal tissues were collected from 28 children with ophthalmorrhexis. None of the patients enrolled in this study had received chemotherapy or radiotherapy prior to surgery. The tissue samples were frozen in the liquid nitrogen and then reserved at −80°C.

Cell Treatment

Human RB cell lines, including Y79 and WERI-Rb-1, were obtained from the American Type Culture Collection cell bank (ATCC, Manassas, VA, USA). Cells were incubated in eagle's minimal essential medium (EMEM) containing 10% fetal bovine serum (FBS) and 1% penicillin/streptomycin at 37°C with 5% CO_2 under 95% saturated humidity. An immunostaining for synaptophysin was conducted to confirm that Y79 and WERI-Rb-1 cells we used were indeed retinoblastoma cells. A synaptophysin specific antibody (ab32127, Rabbit, 1:200; Abcam, Cambridge, UK) was applied for immunostaining. The results are shown in Supplementary Figure S1.

According to the known sequences of let-7a and MST4 obtained from the National Center for Biotechnology Information, the let-7a-mimic, let-7a inhibitor, siRNA against MST4 (si-MST4), and MST4 overexpression plasmid (oe-MST4) were constructed by Shanghai Sangon Biological Engineering Technology & Services Co., Ltd. (Shanghai, China). Briefly, cells were transfected with the aforementioned sequences or plasmids based on the instructions of Lipofectamine 2000 (Invitrogen, Carlsbad, CA, USA).

RNA Isolation and Quantitation

After a 24 hour transfection, total RNA was extracted from tissues or cells with the use of TRIzol reagent (Invitrogen, Carlsbad, CA, USA). Then total RNA (miRNA and mRNA) was reversely transcribed into complementary DNA (cDNA) using TaqMan MicroRNA Reverse Transcription Kit (4366596; Thermo Fisher Scientific, Waltham, MA, USA) and High-Capacity cDNA Reverse Transcription Kit (4368813; Thermo Fisher Scientific), respectively. Real-time quantitative polymerase chain reaction (qPCR) was performed using SYBR Premix Ex Taq (Tli RNaseH Plus) kit (RR820A; Takara Holdings Inc., Kyoto, Japan), with glyceraldehyde-3-phosphate dehydrogenase (GAPDH) and U6 (Invitrogen, Carlsbad, CA, USA) used as the internal references. A real-time fluorescent qPCR instrument (ABI7500; ABI Company, Oyster Bay, NY, USA) was used for PCR. The primers were synthesized by Invitrogen (Table) and the fold changes were calculated by the $2^{-\triangle\triangle Ct}$ method.

Western Blot Analysis

The total protein was extracted from tissues or cells in accordance with the instructions provided on the radio-immunoprecipitation assay kit (R0010; Beijing Solarbio Life Sciences Co., Ltd., Beijing, China). The protein concentration was determined using the bicinchoninic acid kit (GBCBIO Technologies Inc., Guangzhou, Guangdong, China). Next, 10% sodium dodecyl sulfate-polyacrylamide gel electrophoresis was used to isolate 40 μg protein samples, which were transferred onto a polyvinylidene fluoride membrane. Next, tris-buffered saline Tween-20 (TBST) containing 5% bovine serum albumin (BSA) was used to block the membrane at room temperature. Subsequently, the membrane underwent incubation with diluted primary rabbit antibodies against ERK (ab32537, 1: 1000), p38 (ab47363, 1: 1000), c-Jun N-terminal kinase (JNK; ab110724, 1: 1000), p-ERK (ab79483, 1: 1000), p-p38 (ab47363, 1: 1000), p-JNK (ab47337, 1: 1000), MST4 (ab52491, 1: 1000), vascular endothelial growth factor (VEGF; ab184784, 1: 1000), and GAPDH (ab181602, 1: 1000) at 4°C overnight. After receiving three washes with TBST, the membrane was incubated at room temperature with horseradish peroxidase-labeled secondary antibody goat anti-rabbit immunoglobulin G (IgG; ab150077, 1: 1000). The aforementioned antibodies were all obtained from Abcam Inc. Later, the membrane
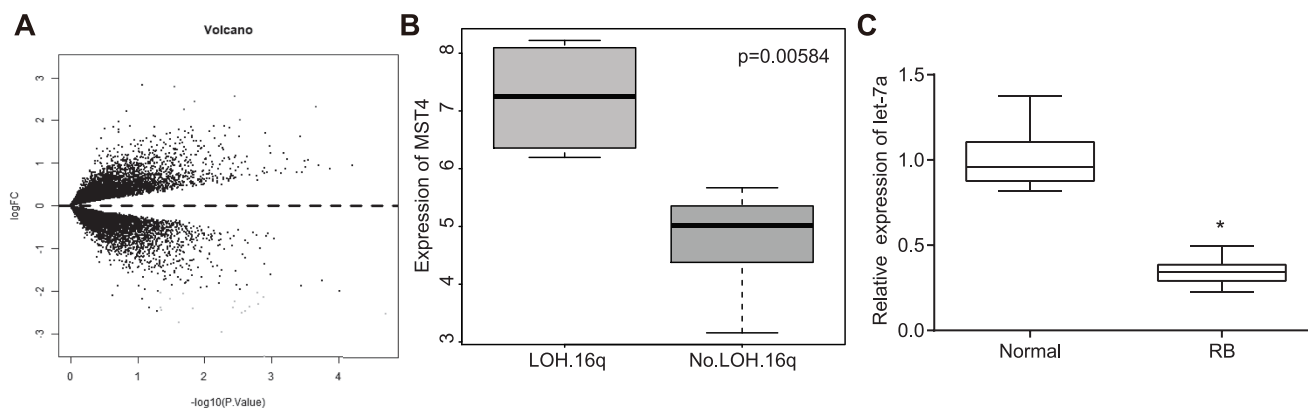
FIGURE 1. MST4 is identified to be upregulated in RB. (**A**) The heatmap of differential expressed genes in RB microarray data. Y-axis represents logFC, and X-axis represents log10 *P* value. Each point indicates one gene, with upregulated gene in red and downregulated gene in green. (**B**) The analysis of MST4 expression in RB samples with or without LOH on 16q from microarray data GSE5222. The gene expression level is represented by Y-axis, whereas grouping information is represented by the X-axis. (**C**) The expression of let-7a in RB tissues determined by RT-qPCR. * $P < 0.05$ compared with normal retinal samples. The above data were measurement data, expressed as mean ± SD, and analyzed by unpaired *t*-test ($n = 28$). RB, retinoblastoma; MST4, Mammalian sterile-20 like kinase 4; MARK, mitogen-activated protein kinase; LOH 16q, loss of heterozygosity on chromosome 16q.

was visualized with a developing solution (NCI4106; Pierce, Rockford, IL, USA). The Image J software was used to determine the gray value of each band, and the ratio of gray value between the target protein band and GAPDH band was calculated.

Immunohistochemistry

The tissue slices were conventionally dewaxed with xylene, and hydrated with anhydrous ethanol, 95% ethanol, and 75% ethanol (each for 3 minutes). The slices underwent incubation with 50 μL 3% H_2O_2 for 20 minutes at room temperature to block endogenous peroxidase activity following antigen retrieval. After being rinsed with phosphate buffer saline (PBS), the slices were incubated with rabbit antibodies against MST4 (ab52491, 1: 500; Abcam Inc.) or VEGF (ab184784, 1: 100; Abcam Inc.) in a 4°C refrigerator overnight. Normal rabbit serum was used as a negative control (NC) to replace the primary antibody. The slices were incubated first with 50 μL polymer reinforcer at 37°C for 20 minutes, and then with 50 μL enzyme-conjugated rabbit antipolymer at 37°C for 30 min. Later, 100 μL newly prepared diaminobenzidine developer was used to develop the slices for 3 to 10 minutes, after which they were observed under a microscope. Finally, the slices were rinsed by distilled water, counterstained by hematoxylin, dehydrated with gradient alcohol (75% ethanol, 95% ethanol, and anhydrous-ethyl), mounted with neutral resin, and observed under a microscope.

Dual-Luciferase Reporter Gene Assay

The target gene of let-7a was predicted based on miRNA.org, and dual-luciferase reporter gene assay was used to validate whether let-7a could directly bind to MST4. Artificially synthesized gene fragment of MST4 3'untranslated region (3'UTR) was inserted into pMIR-reporter (Beijing Huayueyang Biotech Co., Ltd., Beijing, China). Moreover, the mutant sequence in which the potential let-7a binding sites were mutated was also constructed. The recombinant dual-luciferase reporter plasmids MST4-wild type (MST4-

WT) and mutant type (MST4-MUT) were, respectively, co-transfected with let-7a-mimic or NC-mimic into HEK-293T cells (Shanghai Biomart Biotech Co., Ltd., Shanghai, China). Cells were collected and lysed for 48 hours after transfection. According to the instructions provided on the dual-luciferase assay kit (K801-200; BioVision, San Francisco, CA, USA), luciferase activity was detected by Glomax20/20 luminometer (Promega, Madison, WI, USA).

Cell Counting Kit-8

When cells were in the logarithmic growth phase, they were collected and re-suspension into single-cell suspension was carried out at a concentration of 5×10^4 cells/mL. Then, 100 μL cell suspension was seeded into each well of a 96-well plate with 5 parallel wells set in each group. The plate was cultured at 37°C and 5% CO_2 for 24 hours, 48 hours, and 72 hours, respectively. Later, each well was incubated for 1 hour with 100 μL cell counting kit (CCK)-8 solution (Beyotime Biotechnology Co., Ltd., Shanghai, China), 1 hour before the termination of the culture. The optical density value at the wavelength of 490 nm was determined by a microplate reader (BD Biosciences, Franklin Lakes, NJ, USA).

Terminal Deoxynucleotidyl Transferase-mediated 2′-Deoxyuridine 5′-Triphosphate-biotin Nick End-Labeling

Cells were collected, washed with PBS, fixed with 4% paraformaldehyde for 60 minutes, and finally washed again with PBS. Cells were then penetrated with PBS containing 0.1% Triton X-100 for 2 minutes and incubation was carried out with TUNEL solution at 37°C for 60 minutes under dark conditions. Then, cells were mounted with anti-fluorescence quenching solution and observed by a fluorescence microscope (OLYMPUS FV1000; Olympus, Tokyo, Japan). The excitation wavelength ranged from 450 to 500 nm, and the emission wavelength varied from 515 to 565 nm. Apoptotic cells showed green fluorescence. Five visual fields were randomly selected and the number of apoptotic
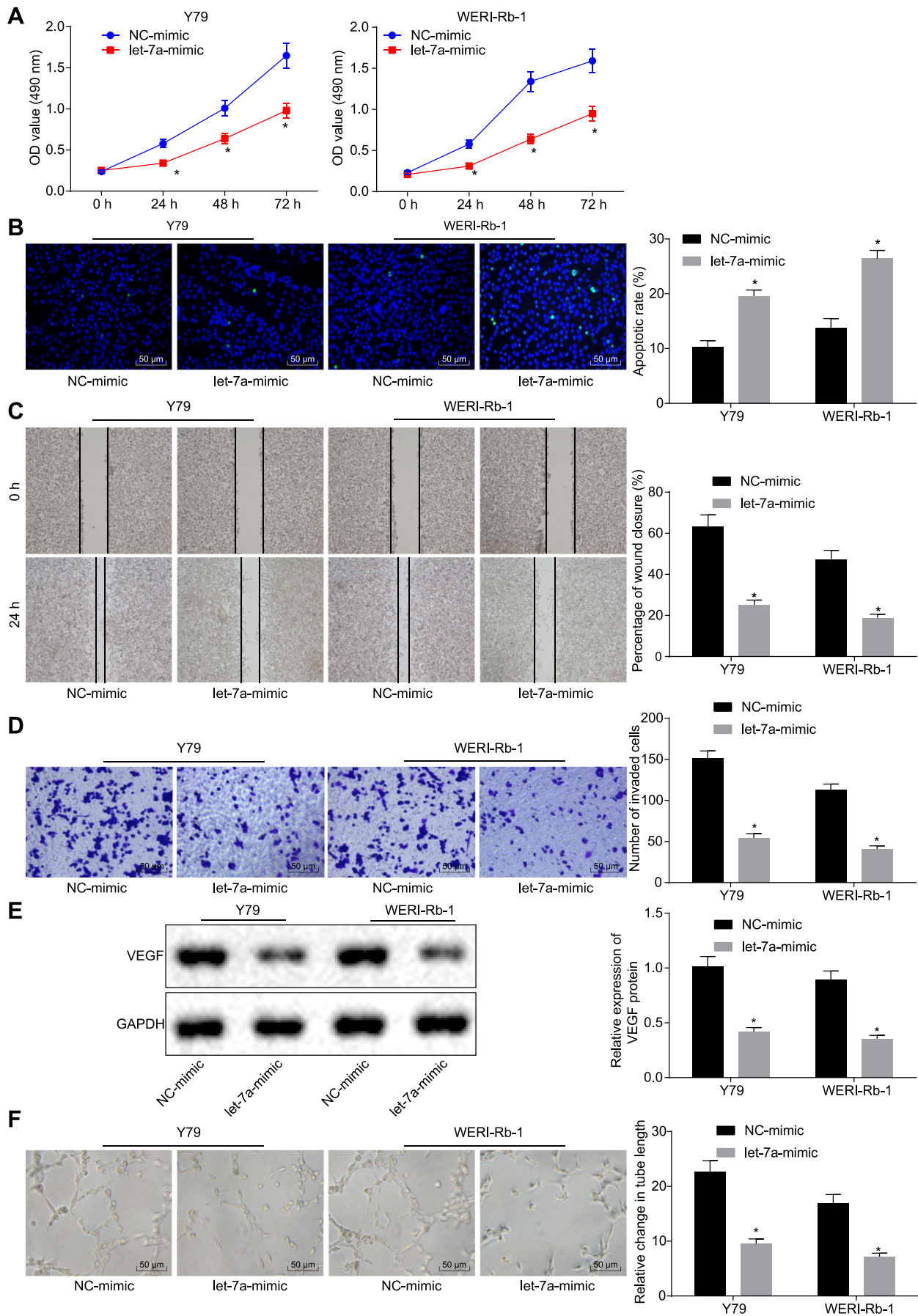
FIGURE 2. Let-7a overexpression represses malignant biological behaviors of RB cells. RB cell lines Y79 and WERI-RB-1 were transfected with let-7a-mimic or NC-mimic for in vitro functional experiments. (**A**) The cell viability at various time points detected by CCK-8 assay. (**B**) The representative images and quantitative analysis of cell apoptosis assessed by TUNEL assay (200 ×, scale bar = 50 µm). (**C**) The representative images and quantitative analysis of cell migration evaluated by scratch test. (**D**) The representative images and quantitative analysis of cell invasion examined by Transwell assay (200 ×, scale bar = 50 µm). (**E**) Western blot analysis of VEGF expression in Y79 and WERI-RB-1 cells normalized to GAPDH. The band intensity was quantified. (**F**) The representative images of in vitro tube formation and the quantitative analysis of the relative length of formed tubes (200 ×, scale bar = 50 µm). * $P < 0.05$ compared with cells transfected with NC-mimic. The results were measurement data, and expressed by mean $\pm$ SD. Unpaired *t*-test was used for the comparisons between the two groups. Repeated measurement ANOVA was utilized for comparisons of data among multiple groups at different time points, followed by Bonferroni post hoc test. Values were obtained from three independent experiments in triplicate. CCK-8, Cell Counting Kit-8; TUNEL, TdT-mediated dUTP-biotin nick end-labeling; RB, retinoblastoma; VEGF, vascular endothelial growth factor; ANOVA, analysis of variance; NC, negative control.

cells was counted. The apoptotic rate was determined using the following formula: apoptotic rate = the average number of positively stained nucleus/all nucleus × 100%.

Scratch Test

Cells were seeded into a 6-well plate at a density of 2.5 × 10^4 cells/cm². The culture medium was removed 24 hours after transfection. Next, the scratches were made with a 100 µL sterile pipette tip. After being washed with PBS, the cells were continually cultured in SmGM-2 culture medium containing 5% FBS. Images of each well were obtained 0 hours and 24 hours post-scratching under an inverted microscope, with 3 duplicated wells set in each group. The width of each scratch was determined by Image J software, and the cell migration ability was detected by comparing the scratch width of each group. Scratch healing rate = (scratch width at 0 hour - scratch width at 24 hours)/scratch width at 0 hour × 100%.

Transwell Assay

After 24-hour transfection, cells were starved in serum-free medium for 24 hours for collection. The cells were resuspended in EMEM containing 10 g/L BSA at a density of 3 × 10^4 cells/mL after receiving two washes with PBS. The Transwell chamber was placed in a 24-well plate. The basolateral Transwell chamber was coated with the Matrigel (40111ES08; Yeasen Company, Shanghai, China) diluted solution (1: 8) and air-dried overnight at 4°C. Cells were resuspended with the culture medium after detachment and PBS washing, and the cell density was adjusted into 1 × 10^5 cells/mL. Then the apical Transwell chamber coated with Matrigel (BD Biosciences) was added with 200 µL cell suspension, and 600 µL culture medium supplemented with 20% FBS was added to the basolateral chamber. Following a 24-hour culture in an incubator with 5% CO_2 at 37°C, the noninvasive cells on the apical chamber were wiped off with a cotton swab. The Transwell chambers were fixed for 15 minutes with 4% paraformaldehyde, stained for 15 minutes by 0.5% crystal violet solution (prepared with methanol), and washed 3 times with PBS. Five visual fields (× 200) were randomly selected and the number of cells that invaded through the membrane was counted using an inverted microscope (XDS-800D; Shanghai Caikon Optical Instrument Co., Ltd., Shanghai, China). Each experiment was conducted in three parallel wells.

Angiogenesis In Vitro

Human umbilical vein endothelial cells (HUVECs) were obtained from the ATCC cell bank (Manassas, VA, USA).

HUVECs were settled on a 24-well plate with 1× 10^5 cells per well, co-cultured with the supernatants of treated RB cell lines (Y79 and WERI-Rb-1) for 24 hours, and then separated.

The 96-well plate was coated with Matrigel (356234; Shanghai Shanran Biotechnology Co., Ltd., Shanghai, China) in an incubator at 37°C for about 30 minutes. Cells were collected 48 hours after transfection and re-suspension was carried out in Dulbecco's modified Eagle's medium after starvation in serum-free medium for 1 hour. The cells at a density of 1 × 10^5 cell/mL were seeded into the 96-well plate coated with Matrigel with three parallel wells in each group. Afterward, the plate was incubated for 18 hours and images were obtained under an inverted phase-contrast microscope (Leica, Inc., Buffalo, NY, USA). Image-Pro Plus (version 6.0) was used to calculate the number of lumens surrounded by cells, and at least three visual fields were counted in each group.

Xenograft Tumor in Nude Mice

Twenty BALB/c nude mice (age: 5–7 weeks; weight: 18–22 g) were purchased from Shanghai Lingchang Biotech Co., Ltd. (Shanghai, China). The mice were acclimated for 7 days in specific pathogen-free environment with a suitable temperature, sterile feed and drinking water, and 12-hour light/darkness cycle in Animal Laboratory Center of Luoyang Central Hospital prior to the experiment. NC-agomir, let-7a-agomir, sh-NC, and sh-MST4 were synthesized by Gene Pharma Company (Shanghai, China). The lentiviruses expressing the aforementioned plasmids were packaged with 293T cells, which were incubated in Roswell Park Memorial Institute-1640 complete medium supplemented with 10% FBS, and passaged every other day. The Y79 and WERI-Rb-1 cells were infected with lentivirus (1 × 10^8 TU/mL) to generate stably infected cell lines. The stably infected Y79 and WERI-Rb-1 cells were made into cell suspension (5 × 10^6 cells/mL). Subsequently, 0.2 mL cell suspension was subcutaneously injected into the right flank of nude mice by 1-mL syringe.[13,14] Tumor formation was observed daily. After 40 days of feeding, the long and short diameters of the tumors were measured with Vernier calipers. Finally, the nude mice were euthanized, and the tumors were removed, photographed, and weighed.

Statistical Analysis

All data were analyzed by SPSS version 21.0 statistical software (IBM Corp., Armonk, NY, USA). Measurement data were expressed in the form of mean $\pm$ SD. Unpaired *t*-test was used for the comparisons between two groups, and one-way analysis of variance (ANOVA) among multiple groups, followed by Tukey's post hoc test. Repeated
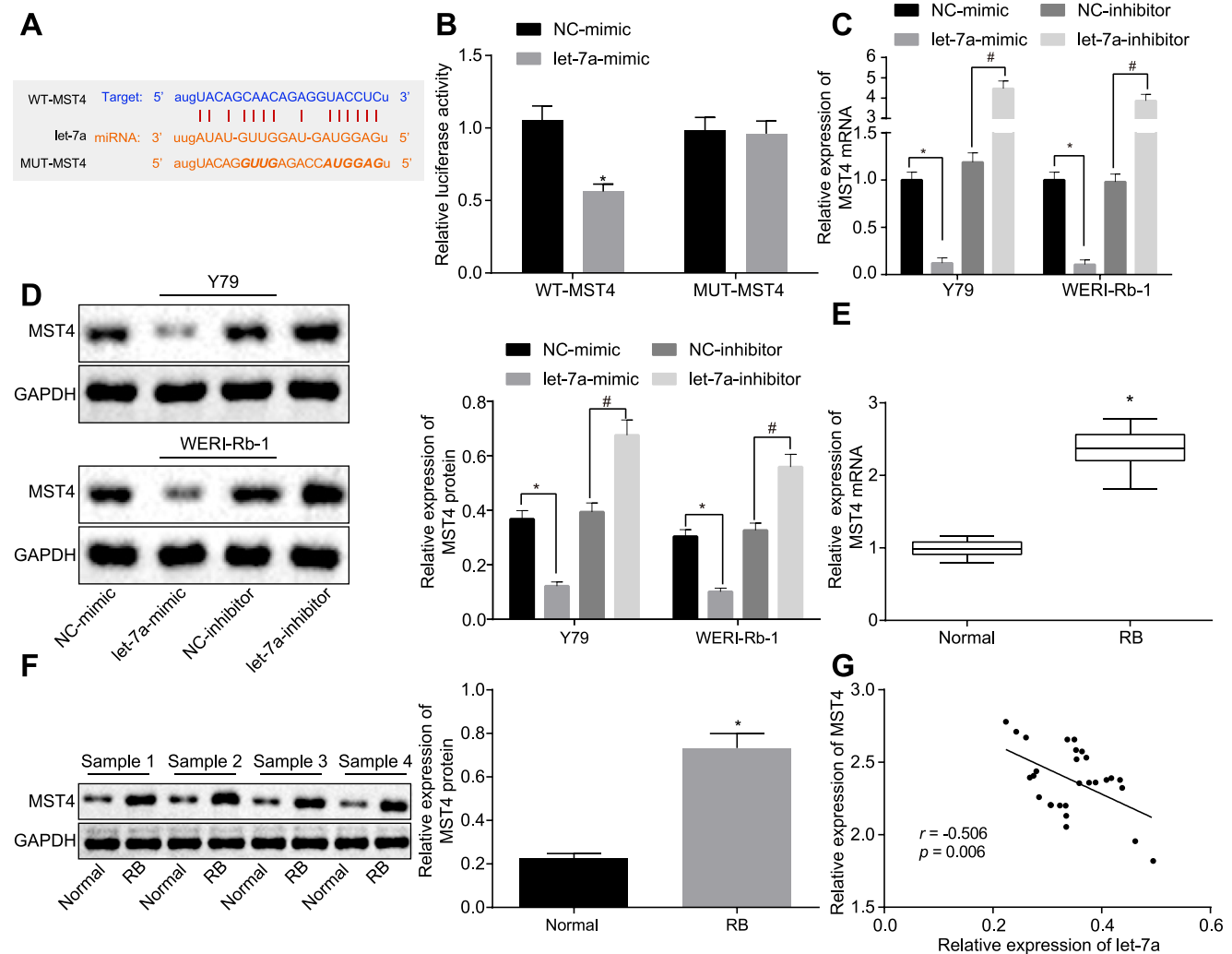
FIGURE 3. Let-7a targets MST4, which exhibits a high expression in RB tissues. (**A**) The binding site of let-7a on MST4 predicted by biological website and mutant sites were shown in bold italic font. (**B**) The binding relationship between let-7a and MST4 verified by dual-luciferase reporter assay. * $P < 0.05$ compared with the co-transfection of NC-mimic and WT-MST4. (**C**) The expression of MST4 in Y79 and WERI-RB-1 cells after transfection with let-7a-mimic or inhibitor determined by RT-qPCR. (**D**) Western blot analysis of MST4 expression in Y79 and WERI-RB-1 cells normalized to GAPDH after transfection with let-7a-mimic or inhibitor. The band intensity was quantified. In panels **C** and **D**, * $P < 0.05$ compared with the treatment of NC-mimic. # $P < 0.05$ compared with the treatment of NC-inhibitor. (**E**) The expression of MST4 in RB tissues and normal retinal samples determined by RT-qPCR ($n = 28$). (**F**) Western blot analysis of MST4 expression in RB tissues and normal retinal samples normalized to GAPDH. The band intensity was quantified ($n = 28$). In panels **E** and **F**, * $P < 0.05$ compared with normal retinal samples. (**G**) Pearson's correlation analysis of the correlation between let-7a expression (data from Fig. 1C) and MST4 mRNA expression (data from Fig. 3E) in RB tissues ($n = 28$). The results were measurement data, and expressed by mean ± SD. Unpaired *t*-test was used for the comparisons between the two groups, and one-way ANOVA was used for the comparisons among multiple groups, followed by Tukey's post hoc test. Pearson correlation analysis was used for between let-7a and MST4 expression. Values were obtained from three independent experiments in triplicate. RB, retinoblastoma; MST4, Mammalian sterile-20 like kinase 4; RT-qPCR, reverse transcription quantitative polymerase chain reaction; NC, negative control.

measures ANOVA was utilized for comparisons of data among multiple groups at different time points, followed by Bonferroni post hoc test. Any *P* values < 0.05 was of significant difference.

RESULTS

MST4 is Identified as a Differentially Expressed Gene in RB

The RB microarray data GSE5222 was obtained from the GEO database, which consisted of 4 RB samples containing loss of heterozygosity on chromosome 16q (LOH 16q)

and 8 RB samples without LOH 16q. Nearly all LOH 16q-deleted RB presented with diffuse intraocular dissemination, suggesting that the changes in the gene located in the microdeletion region were associated with impaired intercellular adhesion.[15] In order to find the differentially expressed genes, microarray analysis was conducted. On the basis of whether LOH 16q was included or not, 25 differentially expressed genes were obtained (Fig. 1A). MST4 was downregulated in the RB samples without LOH 16q and upregulated in the RB samples containing LOH 16q, indicating that MST4 was upregulated in RB and might participate in the RB development (Fig. 1B). In addition, a previous study found upregulated levels of MST4 in pancreatic cancer.[16] The Jeffer-
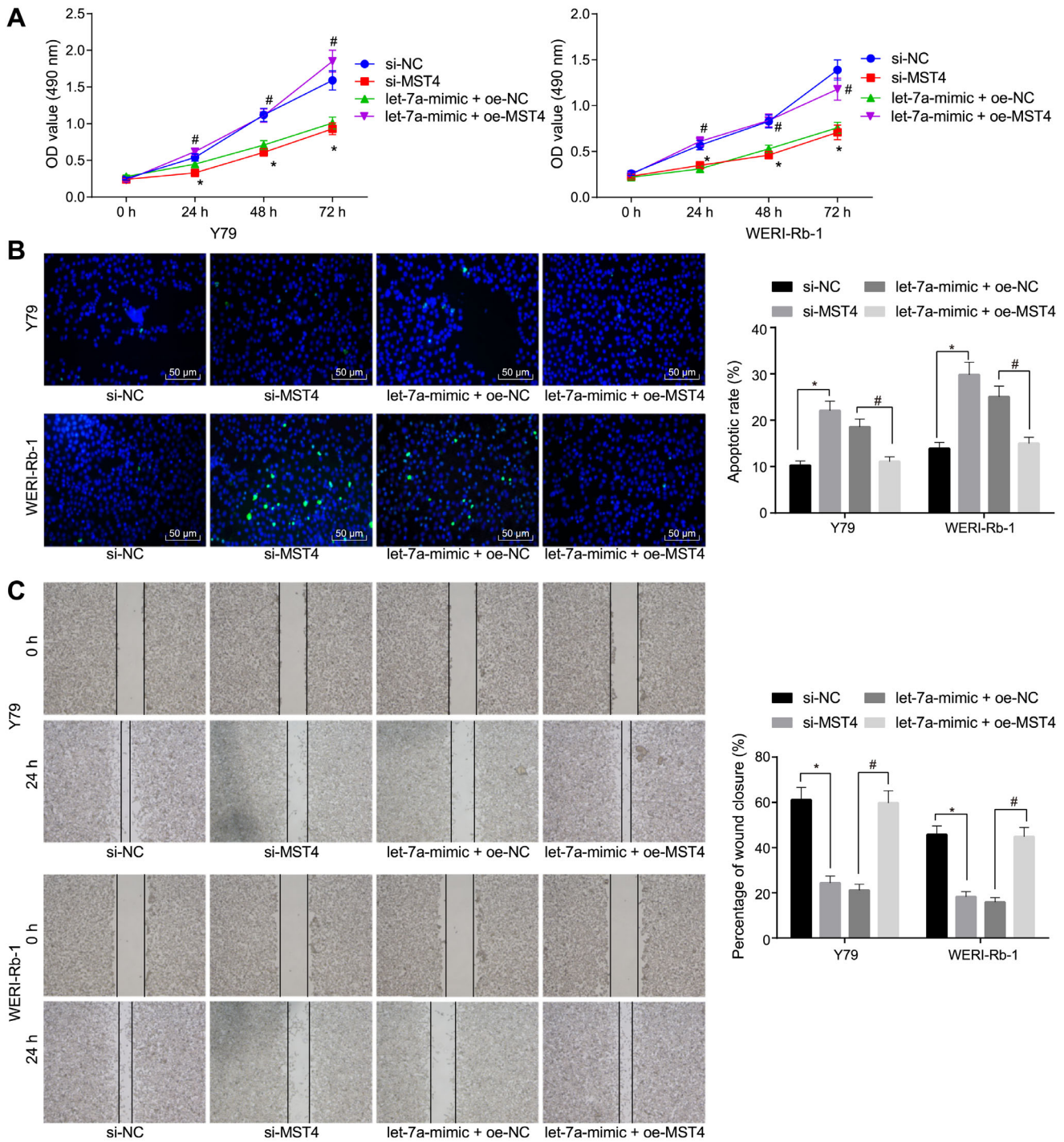
FIGURE 4. Let-7a suppresses malignant biological behaviors of RB cells by negatively regulating MST4. Y79 and WERI-RB-1 cells were transfected with si-MST4 or si-NC, or co-transfected with let-7a-mimic and oe-NC, or let-7a-mimic and oe-MST4. (**A**) The viability of Y79 and WERI-RB-1 cells at various time points assessed by CCK-8 assay. (**B**) The representative images and quantitative analysis of apoptosis of Y79 and WERI-RB-1 cells detected by TUNEL assay (200 ×, scale bar = 50 µm). (**C**) The representative images and quantitative analysis of cell migration of Y79 and WERI-RB-1 cells examined by scratch test. (**D**) The representative images and quantitative analysis of cell invasion of Y79 and WERI-RB-1 cells evaluated by Transwell assay (200 ×, scale bar = 50 µm). (**E**) Western blot analysis of VEGF expression in Y79 and WERI-RB-1 cells normalized to GAPDH. The band intensity was quantified. (**F**) The representative images of in vitro tube formation and the quantitative analysis of the relative length of formed tubes (200 ×, scale bar = 50 µm). * $P < 0.05$ compared with cells transfected with NC-mimic. # $P < 0.05$ compared with cells co-transfected with let-7a-mimic and oe-NC. The above data were measurement data, and expressed by mean ± SD. Unpaired *t*-test was used for the comparisons between the two groups. Repeated measurement ANOVA was utilized for comparisons of data among multiple groups at different time points, followed by Bonferroni post hoc test. Values were obtained from three independent experiments in triplicate. CCK-8, Cell Counting Kit-8; TUNEL, TdT-mediated dUTP-biotin nick end-labeling; RB, retinoblastoma; ANOVA, analysis of variance; NC, negative control.
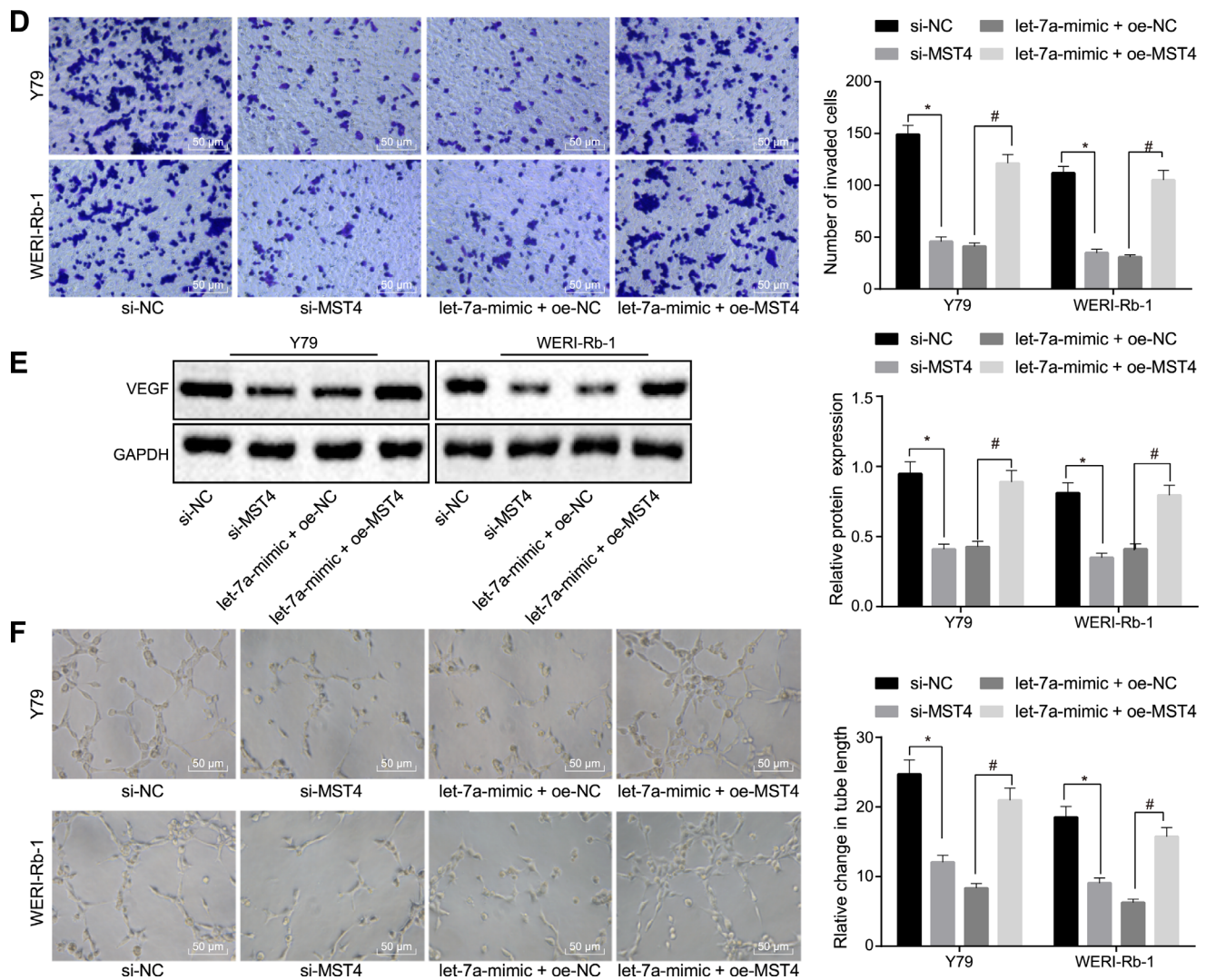
FIGURE 4. Continued.

son database was used to predict the miRNAs that could regulate MST4 and the findings revealed that let-7a was able to target MST4 and downregulate MST4 in RB, which has been reported to be dysregulated in RB according to a prior study.[7] The MST4 gene can regulate the biological function and potential mechanism of the MAPK signaling pathway in the pathogenesis of central nervous system diseases.[10] Combined with the above analysis, let-7a might target MST4 and mediate the MAPK signaling pathway regulating malignant biological behaviors of RB cells. Next, real-time (RT)-qPCR was conducted to determine the let-7a expression in RB, and significantly downregulated levels of let-7a were found in RB tissues ($n = 28$) compared with normal retinal samples ($n = 28$; $P < 0.05$; Fig. 1C). Therefore, let-7a has poor expression in RB.

Let-7a Suppresses Malignant Biological Behaviors of RB Cells

To further study the role of let-7a in RB, let-7a was over-expressed in Y79 and WERI-RB-1 cells, and RB cell migration, viability, invasion, and apoptosis were evaluated follow-ing the overexpression of let-7a. It was found that overexpression of let-7a resulted in decreased viability (Fig. 2A), migration and invasion abilities (Figs. 2C, 2D), along with enhanced apoptosis of Y79 and WERI-RB-1 cells (Fig. 2B). Western blot analysis showed that let-7a overexpression led to an evident decrease in the VEGF expression (Fig. 2E). Angiogenesis assay showed that overexpressed let-7a led to a significant reduction in lumen formation in vitro (Fig. 2F). In conclusion, overexpression of let-7a accelerates apoptosis, and suppresses migration, proliferation, angiogenesis, and invasion of RB cells.

MST4 is One of the Target Genes of Let-7a

As predicted in the biological website, there was a binding site between MST4 and let-7a (Fig. 3A), which was further investigated using dual-luciferase reporter gene assay, which was performed to determine whether MST4 was a target gene of let-7a (Fig. 3B). The luciferase activity of WT-MST4 decreased following co-transfection of let-7a-mimic compared with the transfection of NC mimic ($P < 0.05$), whereas the luciferase activity of MUT-MST4 showed no significant difference following the co-transfection of
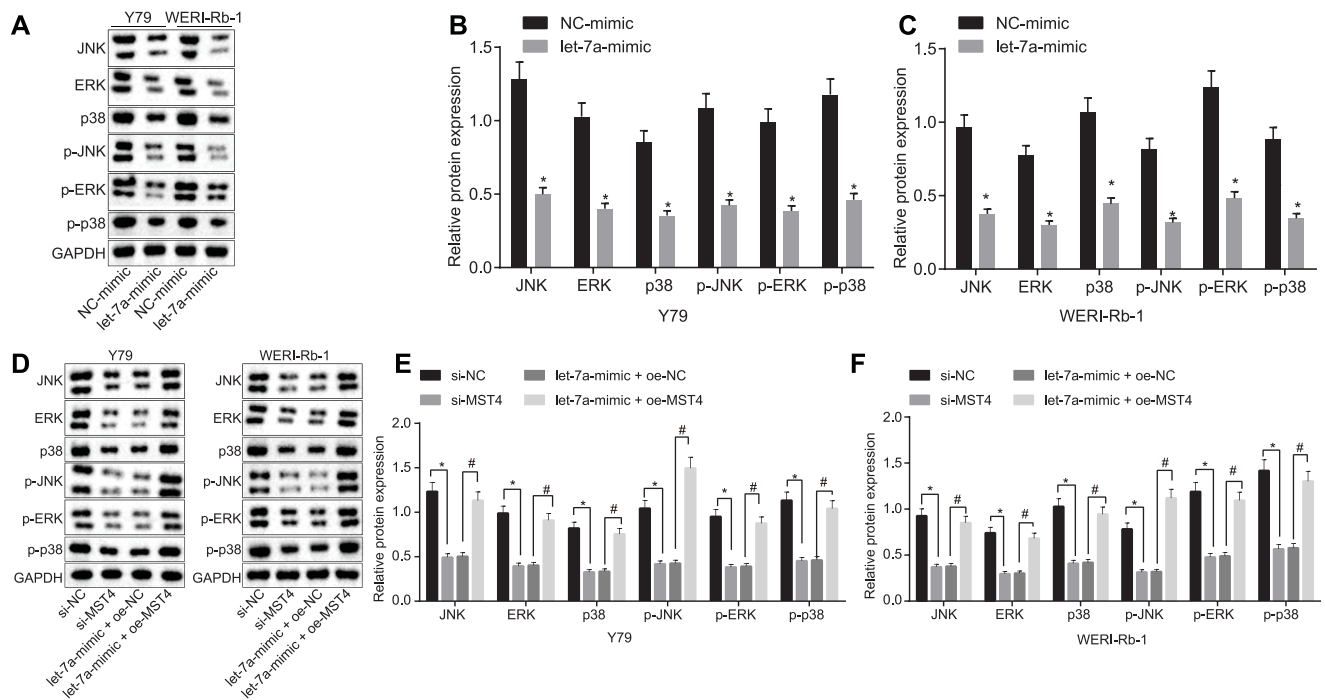
FIGURE 5. Let-7a exerts an inhibitory effect on MAPK signaling pathway by targeting MST4. Y79 and WERI-RB-1 cells were transfected with NC-mimic or let-7a-mimic. (**A**) The gray value of protein bands (JNK, ERK, p38, and JNK, ERK, and p38 phosphorylation) in Y79 and WERI-RB-1 cells. (**B**) The protein expression of JNK, ERK, p38, and the extents of JNK, ERK, and p38 phosphorylation normalized to GAPDH in Y79 cells. (**C**) The protein expression of JNK, ERK, p38, and the extents of JNK, ERK, and p38 phosphorylation normalized to GAPDH in WERI-RB-1 cells. In panels **B** and **C**, * $P < 0.05$ compared with cells transfected NC-mimic. Next, Y79 and WERI-RB-1 cells were treated with si-MST4, si-NC, or co-transfected with let-7a-mimic or oe-NC, or let-7a-mimic and oe-MST4. (**D**) The gray value of protein bands (JNK, ERK, p38, and JNK, ERK, and p38 phosphorylation) in Y79 and WERI-RB-1 cells. (**E**) The protein expression of JNK, ERK, p38, and the extents of JNK, ERK, and p38 phosphorylation normalized to GAPDH in Y79 cells. (**F**) The protein expression of JNK, ERK, p38, and the extents of JNK, ERK, and p38 phosphorylation normalized to GAPDH in WERI-RB-1 cells. In panels **E** and **F**, * $P < 0.05$ compared with cells transfected with si-NC. # $P < 0.05$ compared with cells co-transfected with let-7a-mimic and oe-NC. The above data were measurement data, and expressed by mean ± SD. Comparisons between two groups were analyzed by unpaired *t*-test. Values were obtained from three independent experiments in triplicate. MST4, mammalian sterile-20 like kinase 4; MARK, mitogen-activated protein kinase; JNK, c-Jun N-terminal kinase; ERK, extracellular-signal-regulated kinases; NC, negative control.

let-7a-mimic ($P > 0.05$). Next, RT-qPCR and Western blot analysis were conducted to determine the MST4 expression at both mRNA and protein levels in Y79 and WERI-RB-1 cells. After the transfection of let-7a-mimic, the expression of MST4 decreased, and after the transfection of let-7a inhibitor, it increased ($P < 0.05$; Figs. 3C, 3D). Then MST4 expression was determined in RB tissues, showing that MST4 expression significantly increased in RB tissues ($n = 28$) relative to normal retinal samples ($n = 28$; $P < 0.05$; Figs. 3E, 3F). Moreover, correlation analysis displayed a negative correlation between let-7a expression and MST4 expression in RB tissues (Fig. 3G). The aforementioned findings suggested that let-7a negatively regulates MST4 in RB.

Let-7a Inhibits Malignant Biological Behaviors of RB Cells by Targeting MST4

Y79 and WERI-RB-1 cells were transfected with si-MST4 or si-NC, and co-transfected with let-7a-mimic and oe-NC or co-transfected with let-7a-mimic and oe-MST4 to further investigate the mechanism of let-7a participating in RB progression by targeting MST4. Then, a series of in vitro experiments were conducted to assess cell viability, apoptosis, migration, and invasion. Compared with the matched controls, the transfection of si-MST4 led to decreased cell viability,

migration and invasion abilities, and accelerated apoptosis, whereas the co-transfection of both let-7a-mimic and oe-MST4 resulted in enhanced cell viability, and migration and invasion abilities, but suppressed apoptosis relative to the co-transfection with let-7a-mimic and oe-NC ($P < 0.05$; Figs. 4A, 4B, 4B, 4D). Moreover, protein expression of VEGF was weakened as a result of MST4 silencing, but it was strengthened after co-transfection of both let-7a-mimic and oe-MST4 in comparison with that after co-transfection with let-7a-mimic and oe-NC ($P < 0.05$; Fig. 4E). In addition, the in vitro lumen formation ability was reduced after the silencing of MST4. Additionally, compared with the co-transfection with let-7a-mimic + oe-NC, the co-transfection with let-7a-mimic and oe-MST4 increased the in vitro lumen formation ability ($P < 0.05$; Fig. 4F). In conclusion, let-7a inhibits progression of RB in vitro by targeting MST4.

Let-7a Inhibits the MAPK Signaling Pathway by Targeting MST4 in RB Cells

To further explore the correlation among let-7a, the MAPK signaling pathway and MST4 in RB, NC-mimic, let-7a-mimic, si-MST4, si-NC, let-7a-mimic, and oe-NC or let-7a-mimic and oe-MST4 were introduced into Y79 and WERI-RB-1 cells. Subsequently, Western blot analysis revealed that
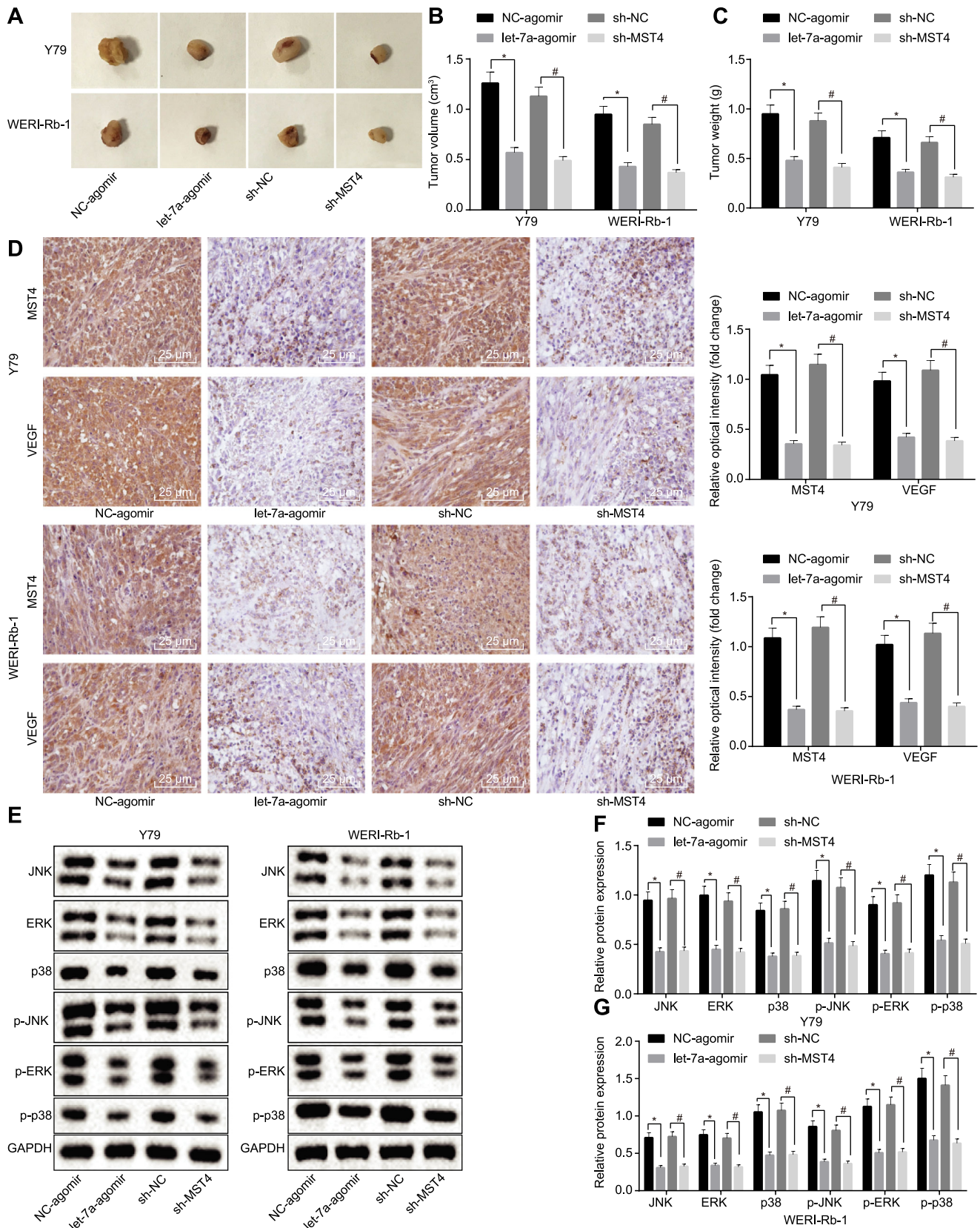
FIGURE 6. Overexpression of let-7a or silencing MST4 represses tumor formation and angiogenesis in vivo. The nude mice were injected with Y79 and WERI-Rb-1 cells stably infected with lentivirus expressing let-7a agomir or sh-MST4 (*n* = 5). (**A**) The representative image of tumors in nude mice 40 days after xenograft transplantation in nude mice. (**B**) The quantitative analysis of the tumor volume in nude mice. (**C**) The quantitative analysis of the tumor weight in nude mice. (**D**) The representative image and quantitative analysis of the expression

of MST4 and VEGF in xenograft tumors detected by immunohistochemistry (400 ×, scale bar = 25 μm). (**E–G**) Western blot analysis of the expression of JNK, ERK, p38, and the extent of JNK, ERK, and p38 phosphorylation in xenograft tumors normalized to GAPDH. The band intensity was quantified. * $P < 0.05$ compared with the treatment of cells stably infected with lentivirus expressing NC-agomir. # $P < 0.05$ compared with the treatment of cells stably infected with lentivirus expressing sh-NC. The above data were measurement data, and expressed by mean ± SD. Comparisons between two groups were analyzed by unpaired *t*-test. MST4, mammalian sterile-20 like kinase 4; JNK, c-Jun N-terminal kinase; ERK, extracellular-signal-regulated kinases; NC, negative control; VEGF, vascular endothelial growth factor.

overexpression of let-7a resulted in a significant decrease of protein expression of JNK, ERK, and p38 and the extents of their phosphorylation ($P < 0.05$), suggesting that let-7a overexpression suppressed the MAPK signaling pathway (Figs. 5A, 5B, 5C). In addition, in contrast to relative controls, the protein expression of JNK, ERK, and p38, and the extents of their phosphorylation decreased after MST4 silencing, and the protein expression of JNK, ERK, and p38, and the extents of their phosphorylation inhibited by let-7a were rescued by restoration of MST4 ($P < 0.05$; Figs. 5D, 5E, 5F). Therefore, based on the above findings, let-7a inhibits the MAPK signaling pathway by targeting MST4 in RB cells.

Upregulated let-7a or Silenced MST4 Suppresses Tumor Formation In Vivo

Finally, in order to assess the role of let-7a and MST4 in tumor growth in vivo, a nude mouse xenograft model of RB was established. The results found that the overexpression of let-7a or silencing MST4 resulted in significant decreases of tumor volume and weight in nude mice (Figs. 6A, 6B, 6C). Furthermore, immunohistochemistry showed that the expression of MST4 and VEGF was reduced following the overexpression of let-7a or silencing MST4 (Fig. 6D). Moreover, Western blot analysis displayed that the expression of JNK, ERK, and p38 and their phosphorylation levels were obviously decreased by either let-7a overexpression or MST4 silencing (Figs. 6E, 6F, 6G). These findings suggest that over-expression of let-7a or silencing MST4 inhibits the MAPK signaling pathway and angiogenesis, thus slowing down the tumor growth in nude mice.

DISCUSSION

RB is the most common eye tumor that often occurs in children, and has a high cure rate.[17] Let-7 has been found to be downregulated in RB.[18] However, further investigations are required to determine the underlying mechanism of let-7a in RB. The current study mainly concentrated on the effects of let-7a on RB and the results found that let-7a overexpression hindered the progression of RB by suppressing MST4-dependent MAPK signaling pathway.

One of the findings in this study showed that MST4 was upregulated in RB tissue and cells. Researchers have demonstrated that when compared with normal pituitaries, MST4 is overexpressed in the human pituitary tumor at both mRNA and protein levels.[19] Furthermore, overexpressed MST4 has been found in highly invasive hepatocellular carcinoma cells and hepatocellular carcinoma spices with vascular invasion.[20] Our study also evidently identified MST4 as a target gene of miR-let-7a, which suppressed the activation of the MARP signaling pathway by downregulating MST4. A functional research has reported that the MAPK signaling pathway can be regulated by miR-4728, a tumor-suppressive miRNA, via MST4,[12] which is similar to the miRNA/mRNA/MAPK regulatory axis from our results. A

previous study suggested that most of the genes in sterile 20 family of kinases, including MST4, are involved in the modulation of MAPK family kinases.[21] MST4 has been particularly indicated as a promotor of ERK/MARK signaling pathway activation, which has been identified as one of the vital factors for cell proliferation.[22] Hence, the above findings suggest that let-7a plays a role in RB by suppressing MST4-mediated MAPK signaling pathway.

Subsequently, our study provided evidence that let-7a is a downregulated miRNA in RB tissues, and its overexpression induced RB cell apoptosis and suppressed cell proliferation, invasion, migration, and angiogenesis, along with a decrease in the expression of VEGF. Other let-7 family members, including let-7b and let-7d, have also been observed to be downregulated in RB tumors in comparison to normal tissues.[18,23] Moreover, several types of cancers have been observed to have decreased expression of let-7a. A previous study has showed downregulated levels of let-7 in lung cancer.[24] Let-7a has also been found to be evidently downregulated in nasopharyngeal carcinoma cells.[25] Furthermore, other members of let-7 families have been identified as potential tumor suppressors against RB.[26] The tumor-suppressive action of let-7a has been documented in a variety of cancers. A recent study demonstrated that in human laryngeal cancer, let-7a plays a role as a potential tumor suppressor.[27] Another study elucidated that the over-expression of let-7a is capable of inhibiting breast cancer cell proliferation, migration, and invasion.[28] Moreover, let-7a plays an anti-angiogenesis effect in mice model of breast tumor.[29] It is well acknowledged that blocking VEGF can lead to the inhibition of angiogenesis and suppression of tumor growth.[30] A prior study showed a significant upregulation in VEGF RB.[31] Hence, our findings suggested that let-7a induced VEGF reduction resulted in the inhibition of angiogenesis in RB, which led to the conclusion that let-7a was an anti-angiogenic regulator. Upregulated levels of MST4 have been found to promote cell proliferation, invasion, and colony formation of hepatocellular carcinoma in vitro.[20] Another study has elaborated that overexpression of MST4 increases both the colony formation ability and rates of cell proliferation in human pituitary tumors that respond to a hypoxic microenvironment.[19] A stable complex of cerebral cavernous malformation 3 and MST4 accelerates cell proliferation and migration synergistically largely via MST4 kinase activation.[32] In this study, we found that overexpression of MST4 could reverse the antitumor effects of let-7a in RB cells. Hence, let-7a inhibited migration, invasion, and angiogenesis but promoted apoptosis of RB cells via targeting MST4.

In conclusion, let-7a inhibited migration, invasion, and angiogenesis but promoted apoptosis of RB cells via blockage of the MAPK signaling pathway by negatively regulating MST4 (Fig. 7). The findings obtained from our study provided further evidence regarding the use of let-7a as a therapeutic target to limit progression of RB. Nevertheless, the feasibility of delivering let-7a or MST4 to human patients with RB in the clinical setting requires further
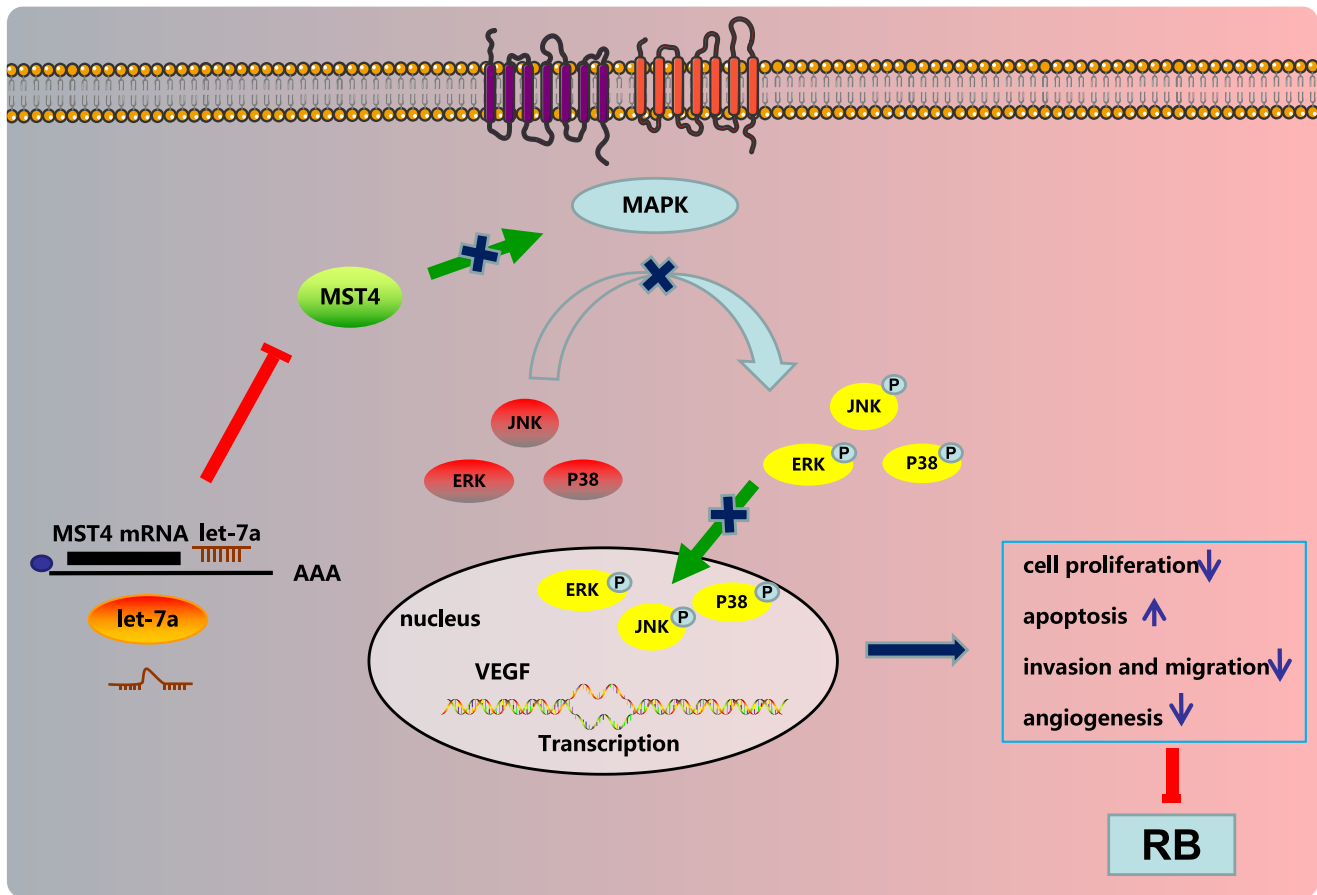
FIGURE 7. Mechanism of let-7a in the regulation of RB progression with involvement of MST4 and the MAPK signaling pathway. Let-7a inhibits MST4 and the MAPK signaling pathway to inhibit proliferation, invasion, migration, and angiogenesis of RB cells and to promote cell apoptosis, thus ultimately repressing RB development.

experiments before application. As our study had time and funding limitations, other mechanisms involved in the MAPK signaling pathway have not been explored yet, which should be the main objective for future studies. In addition, the mechanism of angiogenesis in RB may be multifactorial and very complex, and the precise molecular mechanism underlying the involvement of let-7a in RB requires further investigation.

References

1. Dimaras H. Retinoblastoma genetics in India: from research to implementation. *Indian J Ophthalmol*. 2015;63:219–226.
2. Benavente CA, Dyer MA. Genetics and epigenetics of human retinoblastoma. *Annu Rev Pathol*. 2015;10:547–562.
3. Kent OA, Mendell JT. A small piece in the cancer puzzle: microRNAs as tumor suppressors and oncogenes. *Oncogene*. 2006;25:6188–6196.
4. Golabchi K, Soleimani-Jelodar R, Aghadoost N, et al. MicroRNAs in retinoblastoma: potential diagnostic and therapeutic biomarkers. *J Cell Physiol*. 2018;233:3016–3023.
5. Sung V, Luo W, Qian D, et al. The Ste20 kinase MST4 plays a role in prostate cancer progression. *Cancer Res*. 2003;63:3356–3363.
6. Xiong W, Matheson CJ, Xu M, et al. Structure-based screen identification of a mammalian Ste20-like kinase 4 (MST4) inhibitor with therapeutic potential for pituitary tumors. *Mol Cancer Ther*. 2016;15:412–420.
7. Yang Y, Mei Q. miRNA signature identification of retinoblastoma and the correlations between differentially expressed miRNAs during retinoblastoma progression. *Mol Vis*. 2015;21:1307–1317.
8. Tang R, Yang C, Ma X, et al. MiR-let-7a inhibits cell proliferation, migration, and invasion by down-regulating PKM2 in gastric cancer. *Oncotarget*. 2016;7:5972–5984.
9. Wu A, Wu K, Li J, et al. Let-7a inhibits migration, invasion and epithelial-mesenchymal transition by targeting HMGA2 in nasopharyngeal carcinoma. *J Transl Med*. 2015;13:105.
10. Chen S, Fang Y, Xu S, et al. Mammalian sterile20-like kinases: signalings and roles in central nervous system. *Aging Dis*. 2018;9:537–552.
11. Zhang Q, Cheng Y, Huang L, et al. Inhibitory effect of carboplatin in combination with bevacizumab on human

retinoblastoma in an in vitro and in vivo model. *Oncol Lett*. 2017;14:5326–5332.

12. Schmitt DC, Madeira da Silva L, Zhang W, et al. ErbB2-intronic microRNA-4728: a novel tumor suppressor and antagonist of oncogenic MAPK signaling. *Cell Death Dis*. 2015;6:e1742.

13. Liu B, Pan S, Xiao Y, Liu Q, Xu J, Jia L. LINC01296/miR-26a/GALNT3 axis contributes to colorectal cancer progression by regulating O-glycosylated MUC1 via PI3K/AKT pathway. *J Exp Clin Cancer Res*. 2018;37:316.

14. Li J, Chen J, Wang S, et al. Blockage of transferred exosome-shuttled miR-494 inhibits melanoma growth and metastasis. *J Cell Physiol*. https://doi.org/10.1002/jcp.28234. [published online ahead of print]

15. Gratias S, Rieder H, Ullmann R, et al. Allelic loss in a minimal region on chromosome 16q24 is associated with vitreous seeding of retinoblastoma. *Cancer Res*. 2007;67:408–416.

16. Chen M, Zhang H, Shi Z, et al. The MST4-MOB4 complex disrupts the MST1-MOB1 complex in the Hippo-YAP pathway and plays a pro-oncogenic role in pancreatic cancer. *J Biol Chem*. 2018;293:14455–14469.

17. Weintraub M, Revel-Vilk S, Charit M, et al. Secondary acute myeloid leukemia after etoposide therapy for retinoblastoma. *J Pediatr Hematol Oncol*. 2007;29:646–648.

18. Mu G, Liu H, Zhou F, et al. Correlation of overexpression of HMGA1 and HMGA2 with poor tumor differentiation, invasion, and proliferation associated with let-7 downregulation in retinoblastomas. *Hum Pathol*. 2010;41:493–502.

19. Xiong W, Knox AJ, Xu M, et al. Mammalian Ste20-like kinase 4 promotes pituitary cell proliferation and survival under hypoxia. *Mol Endocrinol*. 2015;29:460–472.

20. Lin ZH, Wang L, Zhang JB, et al. MST4 promotes hepatocellular carcinoma epithelial-mesenchymal transition and metastasis via activation of the p-ERK pathway. *Int J Oncol*. 2014;45:629–640.

21. Lin JL, Chen HC, Fang HI, et al. MST4, a new Ste20-related kinase that mediates cell growth and transformation via modulating ERK pathway. *Oncogene*. 2001;20:6559–6569.

22. Ma X, Zhao H, Shan J, et al. PDCD10 interacts with Ste20-related kinase MST4 to promote cell growth and transformation via modulation of the ERK pathway. *Mol Biol Cell*. 2007;18:1965–1978.

23. Danda R, Krishnan G, Ganapathy K, et al. Targeted expression of suicide gene by tissue-specific promoter and microRNA regulation for cancer gene therapy. *PLoS One*. 2013;8:e83398.

24. Esquela-Kerscher A, Trang P, Wiggins JF, et al. The let-7 microRNA reduces tumor growth in mouse models of lung cancer. *Cell Cycle*. 2008;7:759–764.

25. Cai K, Wan Y, Sun G, et al. Let-7a inhibits proliferation and induces apoptosis by targeting EZH2 in nasopharyngeal carcinoma cells. *Oncol Rep*. 2012;28:2101–2106.

26. Lambertz I, Nittner D, Mestdagh P, et al. Monoallelic but not biallelic loss of Dicer1 promotes tumorigenesis in vivo. *Cell Death Differ*. 2010;17:633–641.

27. Long XB, Sun GB, Hu S, et al. Let-7a microRNA functions as a potential tumor suppressor in human laryngeal cancer. *Oncol Rep*. 2009;22:1189–1195.

28. Kim SJ, Shin JY, Lee KD, et al. MicroRNA let-7a suppresses breast cancer cell migration and invasion through downregulation of C-C chemokine receptor type 7. *Breast Cancer Res*. 2012;14:R14.

29. Isanejad A, Alizadeh AM, Amani Shalamzari S, et al. MicroRNA-206, let-7a and microRNA-21 pathways involved in the anti-angiogenesis effects of the interval exercise training and hormone therapy in breast cancer. *Life Sci*. 2016;151:30–40.

30. Detmar M. Tumor angiogenesis. *J Investig Dermatol Symp Proc*. 2000;5:20–23.

31. Yuan S, Song H. [Expression and clinical implication of matrix metalloproteinase-1 and vascular endothelial growth factor in retinoblastoma]. *Yan Ke Xue Bao*. 2010;25:48–51.

32. Zhang M, Dong L, Shi Z, et al. Structural mechanism of CCM3 heterodimerization with GCKIII kinases. *Structure*. 2013;21:680–688.